



UNLIMITED DISTRIBUTION

DRES

AD-A224 008

SUFFIELD MEMORANDUM

NO. 1321

**A SENSOR STABILIZATION/TRACKING SYSTEM
FOR UNMANNED AIR VEHICLES**

by

Jean-Paul DeCruyenaere

DTIC FILE COPY
JUL 17 1990
CB

May 1990



DEFENCE RESEARCH ESTABLISHMENT SUFFIELD, RALSTON, ALBERTA

WARNING
The use of this information is permitted subject to
recognition of proprietary and patent rights.

Canada

90 07 16 280

UNCLASSIFIED

DEFENCE RESEARCH ESTABLISHMENT SUFFIELD
RALSTON, ALBERTA

SUFFIELD MEMORANDUM NO. 1321

A SENSOR STABILIZATION/TRACKING SYSTEM
FOR UNMANNED AIR VEHICLES

by

Jean-Paul DeCruyenaere



Accession For	
NTIS CRA&I	<input checked="" type="checkbox"/>
DTIC TAB	<input type="checkbox"/>
Unannounced	<input type="checkbox"/>
Justification	
By	
Distribution/	
Availability Codes	
Dist. and/or	
Dart	Serial
A-1	

WARNING
The use of this information is permitted subject to recognition of proprietary and patent rights.

UNCLASSIFIED

UNCLASSIFIED

ABSTRACT

A control algorithm for the automatic steering of an imaging sensor has been developed. Both the tracking of a fixed ground point and the stabilization of the sensor are addressed. This system has been implemented in large part with pre-existing hardware and software in a UAV system. This report describes the theoretical basis of the system as well as detailing the issues concerning the development of a working prototype.

UNCLASSIFIED

UNCLASSIFIED

CONTENTS

Nomenclature	vi
Introduction	1
Background	3
Ground Control Station	3
Air Vehicle	3
Command and Control System	4
Sensor Package	4
Data Links	4
Algorithm	5
Geometry	5
Spotting	6
Tracking	8
Implementation	10
Speed Considerations	10
Accuracy Considerations	11
Numerical Format	11
Alignment	11
Sensor Errors	12
Noise	12
Testing	14
Bench Tests	14
Flight Tests	14
Test Conclusions	14
Future Work	16
Improvement of Pointing Accuracy	16
Heading Error	16

UNCLASSIFIED

Altitude Error	16
Air Vehicle Position and Attitude Error	17
Improved Camera Mount	18
Pegasus IB Autopilot	18
New Algorithm	18
Summary	20
Appendix A	A-1

UNCLASSIFIED

LIST OF FIGURES

1	Surveillance UAV System	22
2	Aircraft Coordinate Notation	23
3	Sensor Geometry	24
4	Overall Geometry	25
5	Spotting Process	26
6	Tracking Process	27

UNCLASSIFIED

LIST OF TABLES

I	Mount Performance	4
II	Execution Times	10

UNCLASSIFIED

UNCLASSIFIED

NOMENCLATURE

Symbol	Description
\vec{C}	the sensor's optical axis
\vec{R}	a scalar multiple of \vec{C}
\vec{G}, G	the tracked ground point
\vec{P}	the air vehicle location
O	the launch site, center of the ground frame of reference (FoR)
X, Y, Z	coordinate axes of the ground FoR
U, V, W	coordinates axes of the AV's FoR
\mathcal{P}, \mathcal{T}	the pan and tilt angles of the sensor mount
L	rotation matrix, ground FoR \Rightarrow AV FoR
M	rotation matrix, AV FoR \Rightarrow ground FoR
Φ, Θ, Ψ	the AV's roll, pitch and yaw angles respectively
$a \dots i$	temporary variables
$A \dots F$	temporary variables
T	control law update period
β	filter constant
τ	effective filter time constant

INTRODUCTION

The Unmanned Vehicle Systems Group (UVSG) at the Defence Research Establishment Suffield conducts research in the area of unmanned air vehicles (UAVs). Within the overall area of UAV's the primary research area of interest to UVSG is command and control, both with respect to the airborne command and control system (ACCS) and the ground control station (GCS) components of an overall UAV system.

Since 1985 UVSG has participated in a number of Canadian Forces exercises by fielding a surveillance UAV system, acting both as a collector of battlefield intelligence and as a forward spotter for artillery fire correction [1, 2]. The experience gained has helped in defining those issues which most critically affect the ability of such a system to collect real-time battlefield information.

One such issue is that of sensor pointing control. The sensor package used to date comprises of a daylight television camera and steerable mount. Until 1987, the control of this sensor package was purely manual, with both the pan and tilt angles of the mount being proportional to the position of a joystick manned by the payload operator (one of three GCS personnel, acting also as image analyst). Great difficulty was experienced by the payload operator due to a lack of sensor stabilization; much of his concentration was required to compensate for small random air vehicle movements while attempting to identify a target. A related problem was the disorientation of the payload operator after the air vehicle had executed a sharp manoeuvre. It was found that the sensor mount was incapable of turning at rates required to keep the target in the field of view.

While the problems mentioned above could be reduced by using a dedicated stabilization system as is currently employed on some existing UAV's [3] these have proven to be heavy and complex. This report will deal with the development of an alternative *distributed* stabilization system, that is one which employs existing sensors and computing resources aboard the UAV. This is the first step in a process of achieving integrated sensor management.

The function of the resulting system will be to compensate for all air vehicle motions, both translational (altitude, northings and eastings) and rotational (pitch, roll and yaw); as such the system will track a fixed ground point as well as pro-

vide some degree of image stabilization. This will allow the payload operator to concentrate fully on the interpretation of the image once he has selected an area to examine, regardless of the air vehicle's flight path or manoeuvring. (For brevity the term "tracking" will be synonymous with compensation for both the rotational and translational motions of the air vehicle; "stabilization" will represent compensation for air vehicle rotations only).

The sensor mount utilized for this work has only two degrees of freedom (pan and tilt); hence it cannot provide compensation for image rotation.

BACKGROUND

The following is a brief description of the UAV system in use during the development of the control system, with emphasis placed on those components which are directly related to sensor steering (Fig. 1).

Ground Control Station

The GCS is comprised of three manned workstations, one each for the air vehicle operator, the mission planner and the payload operator.

The payload operator controls the pan and tilt angles of the sensor through a joystick, either directly or by control of the slew rates. The zoom of the sensor lens can be set to one of eight settings through menu (keystroke) commands, the resulting field of view varying from 4.5° to 20°. The tracking system is activated or deactivated by menu command as well.

At present both the air vehicle and payload operators have some control over the location of the sensor footprint. This leads to control conflicts unless the actions of both operators are somehow coordinated. Currently, this coordination is achieved verbally. Future configurations will implement a form of automatic coordination between the air vehicle path and sensor steering. Footprint-guided flight and automatic footprint sweeping are examples of algorithms which manifest this automatic coordination.

Air Vehicle

A manned surrogate aircraft is currently used as a convenient alternative to an actual UAV airframe. While having different turning rates and speed characteristics, the surrogate acts as a good platform for the testing of avionics and control system hardware and software.

Command and Control System

The Pegasus autopilot [4] is based on an 8 bit microcomputer operating at 1.2 MHz; this is the only computing element present. It handles all of the computing tasks required by the UAV, such as AV stabilization in pitch and roll, telemetry encoding/decoding, sensor steering, engine control and navigation. All of the control laws are updated at 30 Hz.

The primary sensors to the autopilot include a vertical gyro, a three-axis magnetometer, static and dynamic pressure transducers.

Sensor Package

The sensor package consists of a shuttered B&W video camera with zoom lens attached to a mount having two degrees of freedom (Table I). As mentioned earlier, its maximum pan and tilt rates are not sufficient to maintain track while the AV is executing a sharp manoeuvre. In addition, the stringent rate and acceleration requirements for stabilization necessitated the design of an improved mount, to be described later in this report.

	Travel	Rate
Pan	350°	15 deg/sec
Tilt	100°	15 deg/sec

Table I: Mount Performance

Data Links

The uplink and downlink are both 9600 baud data streams consisting of 12 bit data words; the uplink is composed of a 16 word frame repeating at 37.5 Hz, while the downlink is composed of a variable-size frame which allows for selectable update rates ranging from 30 Hz to 0.5 Hz.

The position of the UAV is derived in the GCS from a complementary filter [5] which combines range and azimuth data from a tracking radar with speed and heading data from the UAV. An accurate estimate of the UAV's position is critical for accurate tracking as well as for targeting in general; this method provides data which is more precise than that which could be achieved by one method alone.

ALGORITHM

The tracking of a fixed point on the ground comprises of two processes: the coordinates of the point must be initially determined (hereon referred to as "spotting") and the camera's tilt and pan angles must be continually updated to keep the field of view centered on the point (referred to as "tracking"). The following is a derivation of the algorithms which allow the autopilot to execute these processes.

Geometry

Standard conventions [6] are used for the aircraft's body frame and rotation angles. See Fig. 2. The ground frame of reference is centered at the launch site O , with the X , Y and Z axes pointing North, East and down respectively (Fig 4).

The vector \vec{C} is defined as being a unit vector in the direction of the camera's optical axis. Vector \vec{R} is simply a scalar multiple of \vec{C} ; its length is the distance between the air vehicle's position and the point of intersection of the camera's optical axis with the ground.

$$\vec{R} = |\vec{R}| \vec{C} \quad (1)$$

Vector \vec{P} represents the air vehicle's position in the ground frame of reference, while \vec{G} is simply

$$\vec{G} = \vec{P} + \vec{R} \quad (2)$$

The ground is approximated as a flat plane which is perpendicular to the Earth's local gravity vector. Also, the camera's pan and tilt angles are defined as follows (Fig. 3).

- pan (\mathcal{P}) is the rotation angle of \vec{C} about W measured positive from U to V ,
- tilt (\mathcal{T}) is the angle between \vec{C} and the $U - V$ plane measured positive from the plane to the negative W axis,

- the direction of \vec{C} when $\mathcal{P} = \mathcal{T} = 0$ is that of the U axis.

Spotting

A rotation matrix \mathbf{L} [6] can be used to convert \vec{C} from the ground frame of reference to the air vehicle's (AV) frame:

$$\begin{bmatrix} C_U \\ C_V \\ C_W \end{bmatrix} = \begin{bmatrix} & & \\ & \mathbf{L} & \\ & & \end{bmatrix} \begin{bmatrix} C_X \\ C_Y \\ C_Z \end{bmatrix} \quad (3)$$

where

$$\mathbf{L} = \begin{bmatrix} \cos \Theta \cos \Psi & \cos \Theta \sin \Psi & -\sin \Theta \\ \sin \Phi \sin \Theta \cos \Psi & \sin \Phi \sin \Theta \sin \Psi & \sin \Phi \cos \Theta \\ -\cos \Phi \sin \Psi & +\cos \Phi \cos \Psi & \\ \cos \Phi \sin \Theta \cos \Psi & \cos \Phi \sin \Theta \sin \Psi & \cos \Phi \cos \Theta \\ +\sin \Phi \sin \Psi & -\sin \Phi \cos \Psi & \end{bmatrix} \quad (4)$$

and (Φ, Θ, Ψ) are the aircraft's roll, pitch and yaw angles respectively.

The matrix \mathbf{L} is actually the product of three rotation matrices, one about each body axis:

$$\mathbf{L} = \mathbf{L}_1(\Phi)\mathbf{L}_2(\Theta)\mathbf{L}_3(\Psi) \quad (5)$$

Note that the order of rotations is significant; to determine the orientation of the aircraft which corresponds to a given set (Φ, Θ, Ψ) , the aircraft is first yawed, then pitched, then rolled, each time about the aircraft's body axes and not the ground frame's axes. The gyroscope - magnetometer combination provides values of pitch, roll and yaw which correspond to this ordering.

To find \vec{G} we must first solve Eq. 3 for \vec{C} expressed in the ground frame,

$$\begin{bmatrix} C_X \\ C_Y \\ C_Z \end{bmatrix} = \begin{bmatrix} & & \\ & \mathbf{M} & \\ & & \end{bmatrix} \begin{bmatrix} C_U \\ C_V \\ C_W \end{bmatrix} \quad (6)$$

where M is the inverse of L . Since L is a unitary matrix, its inverse is simply its transpose:

$$M = \begin{bmatrix} \cos \Theta \cos \Psi & \sin \Phi \sin \Theta \cos \Psi & \cos \Phi \sin \Theta \cos \Psi \\ & -\cos \Phi \sin \Psi & +\sin \Phi \sin \Psi \\ \cos \Theta \sin \Psi & \sin \Phi \sin \Theta \sin \Psi & \cos \Phi \sin \Theta \sin \Psi \\ & +\cos \Phi \cos \Psi & -\sin \Phi \cos \Psi \\ -\sin \Theta & \sin \Phi \cos \Theta & \cos \Phi \cos \Theta \end{bmatrix} \quad (7)$$

For brevity, the entries of M will be abbreviated as follows:

$$M = \begin{bmatrix} a & b & c \\ d & e & f \\ g & h & i \end{bmatrix} \quad (8)$$

The vector $\vec{C}_{(AV)}$ can be written in terms of the pan and tilt angles (Fig. 3).

$$\begin{bmatrix} C_U \\ C_V \\ C_W \end{bmatrix} = \begin{bmatrix} \cos T \cos P \\ \cos T \sin P \\ -\sin T \end{bmatrix} \quad (9)$$

Substituting Eq. 9 into Eq. 6 results in

$$\begin{bmatrix} C_X \\ C_Y \\ C_Z \end{bmatrix} = \begin{bmatrix} a(\cos T \cos P) + b(\cos T \sin P) + c(-\sin T) \\ d(\cos T \cos P) + e(\cos T \sin P) + f(-\sin T) \\ g(\cos T \cos P) + h(\cos T \sin P) + i(-\sin T) \end{bmatrix} \quad (10)$$

From Eq. 1 one writes

$$R_X = \frac{R_Z C_X}{C_Z} \quad (11)$$

$$R_Y = \frac{R_Z C_Y}{C_Z} \quad (12)$$

and from Eq. 2

$$\begin{aligned} G_X &= P_X + R_X \\ G_Y &= P_Y + R_Y \end{aligned} \quad (13)$$

The spotting process is shown in Fig. 5. When evaluating the above equations the air vehicle's northings and eastings relative to the launch site O are used for P_X and P_Y . The air vehicle's altitude is substituted for R_Z , which is equal to P_Z due to the flat earth assumption.

Tracking

Eq. 11 can be expanded as follows:

$$\begin{aligned} R_X [g(\cos T \cos \mathcal{P}) + h(\cos T \sin \mathcal{P}) - i \sin T] = \\ R_Z [a(\cos T \cos \mathcal{P}) + b(\cos T \sin \mathcal{P}) - c \sin T] \end{aligned} \quad (14)$$

This can be rewritten as

$$\tan T = \frac{\cos \mathcal{P} [R_X g - R_Z a] + \sin \mathcal{P} [R_X h - R_Z b]}{[R_X i - R_Z c]} \quad (15)$$

Likewise, Eq. 12 can be rewritten as

$$\tan T = \frac{\cos \mathcal{P} [R_Y g - R_Z d] + \sin \mathcal{P} [R_Y h - R_Z e]}{[R_Y i - R_Z f]} \quad (16)$$

For brevity, Eq. 15 will be written as

$$\tan T = \frac{A \cos \mathcal{P} + B \sin \mathcal{P}}{C} \quad (17)$$

and likewise for Eq. 16:

$$\tan T = \frac{D \cos \mathcal{P} + E \sin \mathcal{P}}{F} \quad (18)$$

By equating Eq. 17 and Eq. 18 we can write

$$\mathcal{P} = \arctan \left(\frac{DC - AF}{BF - CE} \right) \quad (19)$$

The final form of this equation has been written with only one division to accommodate a rapid calculation by the autopilot. Once the pan angle has been calculated by the above equation, the tilt angle can be found by returning to either Eq. 17 or Eq. 18.

Solving the above equations results in two possible sets of $(\mathcal{P}, \mathcal{T})$: one which corresponds to \vec{R} , the other which corresponds to $-\vec{R}$. To determine the correct choice, the component of \vec{R} along the W axis is found.

If \vec{C} is replaced with \vec{R} in Eq. 3:

$$R_W = R_X c + R_Y f + R_Z i \quad (20)$$

The decision as to which set to choose is made as follows:

1. if R_W is positive, choose the set with a negative tilt angle,
2. if R_W is negative, choose the set with a positive tilt angle. (As a positive tilt angle is physically impossible for the camera to realize, the tilt is in reality set to zero). This situation may conceivably arise if the target point is far from the aircraft and the aircraft is pitched or rolled in the direction of the target point. The pan angle is nevertheless set correctly, which allows for a quick reacquisition once the target becomes "visible" again.
3. if R_W is close to zero, the choice as to which set to use would have to be based on some other criteria. In this case \vec{R} or $-\vec{R}$ is chosen according to \mathcal{P} ; that vector which results in a value of \mathcal{P} closest to the value computed during the last update cycle is chosen.

Methods (i) and (ii) may produce incorrect results if \mathcal{T} is small in magnitude: R_W will also be small in this case, and could potentially be of the wrong sign due to noise or to the time lag of the overall system. Conversely, method (iii) may produce incorrect results if \mathcal{T} is close to 90° . In this case the rate of change of \mathcal{P} can approach infinity as \vec{C} passes near this point, and a choice based on the smallest change of \mathcal{P} may be erroneous. For these reasons the threshold value of \mathcal{T} used to determine which method is to be used can set arbitrarily to some value which is close to neither 0° nor 90° .

The tracking process is shown in Fig. 6.

IMPLEMENTATION

The above algorithms for spotting and tracking have been used in the writing of two sets of software; one includes the actual assembler code which is meant to be integrated into the existing Pegasus software, along with test versions meant for emulation only. The other includes short PASCAL programs which aid in testing both the validity of the algorithm and the more complex assembler code.

The remainder of this report describes the process of implementing this algorithm into our existing UAV system.

Speed Considerations

Due to the limited amount of processing power available in the autopilot, it was necessary to update the tracking routine at 15Hz, instead of 30Hz as is the case with the remainder of the functions executed.

The computations are performed in the large part with a 24 bit fixed point numerical format, allowing for very fast addition, subtraction and multiplication. In addition to the aforementioned, the only other operations required by the final equations were those of division and arctangent, which were implemented as shown in the appendix. A listing of the execution times required by each operation when run on the Pegasus autopilot is shown in Table II.

Operation	Execution Time
add / subtract	21.2 μ sec
multiply	167.2 μ sec
divide	1.26 msec
arctan	0.60 msec

Table II: Execution Times

Accuracy Considerations

The original performance goal was to achieve pointing accuracy within 1°; while not overly stringent, this nevertheless required attention to certain error sources as listed below.

Numerical Format

As mentioned earlier, the computations are performed in a 24 bit fixed point format; this format represents a fractional value which varies from -1.0 to +1.0. Multiplications will therefore invariably produce results which have an accuracy which is less than or equal to that of the multiplicands. To offset this trend, it is necessary to shift the values, which is done only at certain locations in the software. This "semi floating point" operation is essentially a compromise between the accuracy of floating point and the speed of fixed point operations.

A related problem was the evaluation of Eq. 17 or Eq. 18; both of these will approach the undefined value of 0/0 for certain aircraft and camera orientations. These equations do not both approach the singularity simultaneously, and the problem was thus solved by allowing the software to chose the appropriate one when calculating T .

Alignment

Proper operation of the tracking system depends on the alignment of a subset of the equipment onboard the AV, namely the magnetometer, the vertical gyroscope and the camera mount. These devices can be thought of as each measuring a vector in space (the local geomagnetic field, gravity and \vec{C} respectively); these vectors must be measured in the same coordinate frame. If this cannot be easily accomplished through the construction of the mounting hardware, it can be done by rotating the data in the autopilot software. This method is used in the case of the magnetometer, which is mounted in the tip of a wing with a significant dihedral and sweep-back angle. The rotation angles needed were determined with precise surveying of the gyroscope and magnetometer sites.

Note that the problem of wing flexure during flight had not been addressed. This flexure can be thought of as having two components: a fixed amount observed during steady, level flight, and a variable component arising due to manoeuvres (both being significant when using a surrogate aircraft). The rotation imparted to the magnetometer by the fixed component can in principle be deduced from data recorded during flight. In practice this problem may not occur depending on the location of the magnetometer and on the type of aircraft used.

Sensor Errors

The specified performance of both the gyroscope and magnetometer used indicates that these sensors would not be the source of significant tracking errors.

The use of a static pressure transducer as an altimeter was originally intended for general flight control. In the case of tracking, the multiple inaccuracies inherent in this form of altimeter, some of which are listed below, can produce a significant tracking error:

- the temperature sensitivity of both the transducer and its reference voltage,
- local pressure changes at the static port due to the AV's aerodynamics,
- pressure changes due to changing meteorological conditions,
- differences between the elevation of the UAV's launching point (the "flat earth" reference elevation) and that of G .

Some efforts were made to control the temperature sensitivity of the altimeter; other altimeter issues are discussed in the remainder of this report.

The positional errors inherent to the camera mount can be controlled during its construction if attention is paid to the alignment of the pan and tilt axes, the alignment of the camera within the mount, the quality of the readout devices, etc.

Noise

To avoid gross errors in the estimate of \vec{R} due to sporadic noise, an average value is derived from multiple spottings. The number of spottings involves a trade-off between the noise-induced error and the error due to camera drift during the spotting series.

The noise present on all of the many input signals to the tracking routine necessitated the inclusion of filtering. First order pole filters (IIR) were applied to the output of the track routine:

$$Y[n] = (1 - \beta)Y[n - 1] + \beta X[n] \quad (21)$$

where the time constant τ is

$$\tau = \frac{-T}{\ln(1 - \beta)} \quad (22)$$

Here $T = 1/30$ sec. and $\beta = 1/8$, resulting in a time constant of 0.25 sec. The time lag introduced by the large value of τ is obviously a limiting factor in the tracking system's bandwidth. Reduction of the noise present on all input signals would allow for a reduction in the amount of filtering in the tracking routine, which in turn may increase the responsiveness of the overall system, depending on which component has the dominant time constant: filter, mount or otherwise.

An analysis of the sensitivity of the complete system to noise, both steady-state and time-varying, will not be presented here; suffice it to say the sensitivity is generally a non-linear function of a subset of the input values. Some of the more important examples are listed below.

The tracking routine is most sensitive to noise in the following cases:

- When flying near G , the routine is sensitive to noise in all components of the estimate of the air vehicle's position (P).
- When flying directly above G or nearly so, the routine is sensitive to noise in the estimation of the AV's northings and eastings (P_X and P_Y), but only in the calculation of \mathcal{P} , which results in random image rotation. Nevertheless, the actual tracking accuracy is not affected.

The spotting routine is sensitive to noise in the estimates of both the air vehicle's attitude (Φ, Θ, Ψ) and altitude (P_Z) when either R_X or R_Y are large in comparison to R_Z .

TESTING

Bench Tests

The validity of the algorithm was first determined with simple simulations using the PASCAL version. Here attention was paid to agreement between the spotting and tracking routines. The numerical accuracy of the assembly language version was determined by comparing its results with that of the PASCAL version. Finally, the assembly language code was integrated into the Pegasus autopilot, which was tested with simulated sensor data.

Flight Tests

The operation of the tracking system was observed to be essentially correct during a series of flight trials. Nevertheless, the system was not used by GCS personnel during Canadian Forces exercises in 1988 and 89, preferring instead the manual control mode. The specific problems which were noted at the time include:

- The pointing accuracy was not sufficient to keep G in the field of view (4.5°) of the camera when high magnification was used. High magnification was used by the payload operator when attempting to identify individual targets.
- Serious tracking errors would occur in the case of loss of air vehicle position data due to errors in the uplink telemetry.
- Difficulty was experienced by the payload operator when attempting to relocate G to another target. Once again this was done at high magnification, whereby the small random motions of the air vehicle would cause large motions in the FoV. The tracking system was unable to compensate for these motions (with frequencies above 2 Hz and amplitudes greater than 1°).

Test Conclusions

The performance achieved by the tracking system was found to be very dependent on both i) the quality of the input data and ii) the ability of the sensor

mount to respond quickly to positioning commands. Both of these points are specific to the particular implementation, and as such are not due to the correctness of the algorithm, nevertheless they must be addressed.

In addition, it may be possible to improve the usefulness of the tracking system by modifying the algorithm such that user-commanded corrections can be applied without the loss of stabilization.

Methods of improving i) and ii), as well as the modified tracking algorithm are discussed in the following chapter.

FUTURE WORK

Improvement of Pointing Accuracy

The final pointing accuracy of the tracking system is largely based on the accuracy of each input data stream. This section discusses the nature of the more important errors in the input data, along with potential improvement methods. Accuracy improvements are also inherent in the use of the modified autopilot and camera mount, described later in this chapter.

Heading Error

The calculation of the AV's heading is very sensitive to any misalignment between the magnetometer and vertical gyro. This is due to the fact that the geomagnetic field is close to vertical at northern latitudes, and that heading is determined by the horizontal component. More accurate heading estimates could be achieved by the relocation of the magnetometer to a more rigid location on the airframe, as well as by fusing with rate gyro data. As an extreme, it may be necessary to model wing flexure within the autopilot and thereby estimate the needed rotation.

Altitude Error

Errors due to the altimeter are potentially significant. These errors can be separated into two categories: errors due to the flat earth assumption, and sensor errors.

The "flat earth" error can further be broken into an error due to the Earth's curvature, and an error due to local terrain elevation changes within the UAV's operating radius. A barometric altimeter (which provides P_Z) does not have an error associated with the Earth's curvature; nevertheless the assumption that $P_Z = R_Z$ is no longer valid. The resulting error ($P_Z - R_Z$) is negligible when the horizontal component of \vec{R} is 10 Km or less.

Local elevation changes are typically in the order of hundreds of meters over the area covered by a short-ranged UAV. This error can be compensated for with a digital terrain elevation map, stored either in the GCS or the UAV. As an alternative,

an active altimeter could be used, such as a radar altimeter or laser rangefinder. In the case of a radar altimeter or similar sensor, the altitude of the air vehicle over the local terrain would be known precisely, yet there would remain an unknown difference between the elevation of G and that of the terrain directly below the air vehicle (S). This error would tend to increase with the distance $G - S$. A laser rangefinder, mounted collinearly to the imaging sensor, would provide an accurate estimate of each component of \vec{R} . If the laser rangefinder was the only source of altitude data, it would be necessary to assume that tracking was precise, and that any changes in $|\vec{R}|$ were due changes in the AV's position. This could lead to an unstable tracking system.

If it is assumed that the barometric altimeter used is sufficiently accurate, weather-related changes in pressure become the primary sensor error for long duration flights. As with the magnetometer, it may be possible to improve the signal with compensations, such as with barometric data measured at the GCS.

The best estimate of R_z would be obtained with a combination of sources, such as a radar altimeter used in conjunction with a terrain elevation map, or a laser rangefinder used with a barometric altimeter.

Air Vehicle Position and Attitude Error

As mentioned earlier, poor quality uplink can produce tracking errors, in this case by way of corrupted air vehicle position data. This and similar uplink problems can be reduced with the use of an onboard model of the AV flight dynamics (essentially a short term navigation system). The AV position as predicted by the model would be used in the case that there is a large disagreement between it and the position data arriving on the uplink.

Work is currently underway at DRES to apply a differential Global Positioning System (DGPS) in a surveillance UAV [7]. Apart from benefits such as increased AV range and autonomy, a DGPS system could provide navigation data including altitude, accurate to within 5 meters, which is an obvious improvement over that available from tracking radars and our current altimeter. Work is also underway to integrate a strapdown AHRS system into the avionics suite so as to achieve a more precise estimate of the AV's attitude.

Improved Camera Mount

The next flights will incorporate a modified camera mount. Its main improvements over the previous mount are:

- much improved slew rates in both axes (minimum 60 deg/sec),

- angular accelerations of 300 deg/sec²,
- continuous 360° travel in pan,
- precise construction necessary to ensure proper alignment,
- accurate position encoders,
- the potential for conversion to fully digital control.

An overall betterment in the tracking accuracy should result, as well as improved stabilization. This mount is in the prototype stage and will require test flights to ascertain its full usefulness.

Pegasus IB Autopilot

A modified version of the Pegasus autopilot is currently being developed to address the limitations of memory and computation capabilities which were encountered during the development of the tracking algorithm. These modifications result in:

- an increase in clock speed from 1.22 to 1.852 MHz, improving computational speed by over 50 %,
- increased RAM (8 Kbytes) and EPROM (64 Kbytes),
- an improved stable reference voltage for use with the altimeter.

New Algorithm

It has been noted that the payload operator experiences difficulty when re-positioning the camera from one ground point to another, mainly due to the lack of any stabilization during this transition. As a result it would be desirable to implement an algorithm which provides stabilization continuously, and not only during tracking mode as has been the case. A possible solution is outlined below:

1. Upon entry into the stabilization mode, use \mathcal{P} , \mathcal{T} and (Φ, Θ, Ψ) to produce a unit vector \vec{C} with respect to the ground frame of reference.
2. Use the pan command to modify the azimuth of \vec{C} in the ground FoR; likewise use the tilt command to modify the elevation of \vec{C} . The commanded values will be derived from the summation of two weighed components, one from the joystick and the other from the tracking algorithm (if selected).

3. Use the newly modified \vec{C} , as well as the present (Φ, Θ, Ψ) to produce the pan and tilt positioning commands for the camera mount.
4. Repeat (ii) through (iv).

This method involves the interpretation of joystick commands as movements in the ground FoR instead of in the air vehicle FoR as before, which may prove more intuitive to the payload operator. Secondly, the joystick commands can be thought of as corrections to the location of G ; this would give the payload operator the ability to select multiple targets in quick succession while retaining the benefits of tracking.

SUMMARY

An algorithm has been developed which allows for the automatic tracking of a fixed ground point using our existing avionics suite and video camera payload. This algorithm has been implemented in the Pegasus autopilot and tested during several flights aboard a surrogate UAV. While the basic operation of the tracking mode was observed to be correct, the poor precision and speed of the system resulted in limited usefulness. These problems will be addressed in the short term with an improved camera mount and autopilot, and in the long term with advanced navigation systems such as the Global Positioning System.

BIBLIOGRAPHY

- [1] Weiler, D.R., Juneau, Capt. J.A.F.J., et al, "RPV Concept Evaluation - RPVs in RV 85 (U)", Suffield Memorandum 1156, February 1986. UNCLASSIFIED
- [2] Chesney, R.H. and Henders, M.G., "Operational Tests of RPVs in Exercise RV 87 (U)", Suffield Report 502, August 1988. UNCLASSIFIED
- [3] Amick, G.S., "Unmanned Air Vehicles Payloads and Sensors", Lockheed Missiles & Space Company, Inc., Lockheed Austin Division, Austin Texas, presented at the AGARD Guidance and Control Symposium, San Francisco, October 1988.
- [4] Burton, S.K. and Weiler, D.R., "The Pegasus Autopilot for Remotely Piloted Vehicles (U)", Suffield Memorandum No. 1167, April 1986. UNCLASSIFIED.
- [5] Aitken, V., "A Complementary Tracking Filter for Remotely Piloted Aircraft (U)", Suffield Memorandum No. 1292, June 1989. UNCLASSIFIED.
- [6] Etkin, B., Dynamics of Atmospheric Flight, John Wiley & Sons, Inc., New York, 1972, Chapter 4.
- [7] Ollevier, T.E., private communication.

APPENDIX A

ARCTAN is implemented as the reverse look-up of a tangent table; a direct look-up of an arctangent table would not have been feasible as the high non-linearity of the function would have caused a loss of resolution in the table for small angles.

DIVX is implemented as two 16 bit integer divisions which, although not as precise as a full 24 bit division, is much faster, due in great part to a 16 bit transfer instruction available to the 63701 microcomputer. The first division is quotient/divisor, which produces a remainder, the second is remainder/divisor. Some further clarification is required to explain the two following operations:

- The 24 bit format is generally used to represent a signed fractional value which varies from -1.0 to $+1.0 - \epsilon$, where $\epsilon = 2^{-23}$.
- This value may include an implied exponent which is some power of 2, depending on its use in the program.
- To produce an output which is precise to within 0.5° , the arctangent function need only accept arguments with a magnitude less than 127; arguments with implied exponents of 2^8 are thus properly formatted for this function, being that they will have the greatest possible resolution while encompassing the necessary range.
- The result of a division is always used as the argument for an arctangent, hence its result should have an implied exponent of 2^8 .

```

*****
*
*           DIVX
*
* THIS PROGRAM IS A DOUBLE 16-BIT DIVIDE
* WHICH PRODUCES A 16-BIT RESULT. THIS RESULT
* IS BOTH SHIFTED RIGHT 8 TIMES AND LIMITED
* TO A VALUE OF 7F (127).
*
* syntax such as " value -> C " denotes the contents of a register,
* while " (value) -> C " also implies that the contents happen to
* be inconsequential to the program.
*
*****
LINE0    BNE    SKIP1           is the divisor = 0 ?
         LDAA  #OFFH
         STAA  DIV_FLG         yes, set error flag and return.
         RTS
SKIP1    CLR    DIV_FLG         no, clear the error flag.
         CLR    SIGN           SIGN records the sign of the quotient.
         TSTA  LINEA           is the divisor negative ?
         BPL   LINEA           if so, negate both the divisor
                                and the sign flag.
         COMA
         COMB
         ADDD  #1
         COM   SIGN
LINEA    STD   DIVISOR
         LDD   V_ACC
         BPL   LINEB           is the dividend negative ?
         COMA           if so, negate both the dividend
         COMB           and the sign flag.
         ADDD  #1
         COM   SIGN
LINEB    JSR   B_ROLLS         do a 16 bit divide, V_ACC / DIVISOR.
         TSTA
         BPL   LINE5
         ADDD  DIVISOR         adjust remainder (step 2, p. 267).
*****
* this section limits the absolute value of the result to 7F (127);
* i.e. a quotient greater than 127 is considered to be approx. 127.
*****
LINE5    IGDY           quot. -> D   rem. -> X

```

```

TSTA
BEQ SKIP2          are 8 m.s. bits of quotient = 0 ?
TST SIGN          no, should the result be positive ?
BPL LINEC
LDD #8000H        no, set V_ACC to -1.
BRA LINED
LINEC LDD #7FFFH   yes, set V_ACC to +1.
LINED STD V_ACC
CLR V_ACC+2
RTS              return to main program.
*****
SKIP2 STAB V_ACC  yes; store the 8 l.s. bits of the
*          quotient into V_ACC.
*****
* this section shifts the remainder up by either 8 or 4 or not at
* all, whichever is the highest possible. It then shifts the
* divisor accordingly until it has been shifted 8 bits down w.r.t
* the remainder.
*****
XGDX          (quot). -> X   rem. -> D
BITA #0FOH    can the remainder be shifted up by 4 ?
BNE LINE6     no; ( shift divisor down 8 ).
ASLD          yes; shift 4.
ASLD
ASLD
ASLD
BITA #0FOH    can the remainder be shifted up again ?
BNE LINE7     no; ( shift the divisor down 4 ).
ASLD          yes; shift 4 a second time.
ASLD
ASLD
ASLD
JSR B_ROLLS   divide the remainder by DIVISOR.
BRA LINE8
LINE6 XGDX     (quot.) -> D   rem. -> X (store rem.)
LDD DIVISOR
LSRD
LSRD
LSRD          shift divisor down 8,
LSRD
LSRD

```

```

        LSRD
        LSRD
        ADDD #1                and round up.
        STD  DIVISOR
        XGDY                    (quot.) -> X  rem. -> D
        JSR  B_ROLLS            divide the remainder by DIVISOR.
        BRA  LINE8
LINE7   XGDY                    (quot.) -> D  rem. -> X (store rem.)
        LDD  DIVISOR
        LSRD
        LSRD                    shift divisor down 4,
        LSRD
        LSRD
        ADDD #1                and round up.
        STD  DIVISOR
        XGDY                    (quot.) -> X  rem. -> D
        JSR  B_ROLLS            divide the remainder by DIVISOR.
*****
LINE8   XGDY                    quot. -> D   (rem.) -> X
        STAB V_ACC+1            store 8 l.s. bits of the quotient
*                                     into V_ACC+1. Note that the 8 m.s.
*                                     bits will always be 0 in this case.
        TST  SIGN                should the final result be negative ?
        BPL  LINE9
        LDD  V_ACC
        COMA
        COMB
        ADDD #1
        STD  V_ACC                yes; negate V_ACC, V_ACC+1.
LINE9   CLR  V_ACC+2            always clear V_ACC+2.
        RTS
*****
* the barrel roll subroutine assumes that the dividend is in
* the D accumulator and divisor is in DIVISOR. It returns the
* quotient in the X register and the remainder in the D register.
* See Computer Organization (McGraw Hill) p. 267 for details on
* the non-restoring integer division algorithm.
*****
B_ROLLS XGDY                    dividend -> X (Q)
        LDAA #16
        STAA COUNT                initialize count to 16 (= # of bits).
        CLRA

```

```

LOOP      CLRB                clear D register. (A)
          TSTA                is "A" positive ?
          BMI   LINE1
          IGDY                yes;  A -> X  Q -> D
          ASLD                shift Q
          IGDY                A -> D  Q -> X
          ROLB
          ROLA                shift A
          SUBD  DIVISOR       subtract M
          BRA   LINE2
LINE1     IGDY                no;   A -> X  Q -> D
          ASLD                shift Q
          IGDY                A -> D  Q -> X
          ROLB
          ROLA                shift A
          ADDD  DIVISOR       add M
LINE2     TSTA                is A positive ?
          BMI   LINE3
          IGDY
          ORAB  #01H          set Q0 to 1.
          IGDY
          BRA   LINE4
LINE3     IGDY                no;
          ANDB  #0FEH         set Q0 to 0.
          IGDY
LINE4     DEC   COUNT         decrement count.
          BNE  LOOP          loop back.
          RTS

```

```

*****
*
*           ARCTAN
*
* ARCTAN IS A REVERSE LOOK-UP OF TAN_TBL.
* IT RETURNS AN ANGLE BETWEEN -PI/2 AND
* +PI/2, EXPRESSED IN RADS/8. THE ARGUMENT
* OF THIS MACRO IS UNDERSTOOD AS HAVING AN
* EXPONENT OF 2^8.
*****
ATN      LDD   V_ACC
          STD  TAN

```

```

      BMI    TH_Q4
      BSR    ATAN
      RTS
TW_Q4  COMA
      COMB
      ADDD  #1
      STD   TAN
      BSR    ATAN
      LDD   V_ACC
      COMA
      COMB
      ADDD  #1
      STD   V_ACC
      RTS
*****
ATAN   LDX   #TAN_TBL
      STX   TH_LASTX
      CLR   RESULT
      LDAB  #80H
ATAN1  STAB  DELTA
      ABX
      ABX
      LDAA  TAN
      CMPA  0,X
      BLO   ATAN3
      BHI   ATAN2
      PSHA
      LDAA  TAN+1
      CMPA  1,X
      PULA
      BLO   ATAN3
ATAN2  STX   TH_LASTX
      ADDB  RESULT
      STAB  RESULT
      BRA   ATAN4
ATAN3  LDX   TH_LASTX
ATAN4  LDAB  DELTA
      LSRB
      BEQ   DONE_ATN
      BRA   ATAN1
DONE_ATN LDAA  RESULT
      CLR  B
```

UNCLASSIFIED

LSRD
LSRD
STD V_ACC
MULX P3927CS
RTS
TAN_TBL FDB 0000H,0001H,0002H,0002H,0003H,0004H,0005H,0006H
FDB 0006H,0007H,0008H,0009H,0009H,000AH,000BH,000CH
FDB 000DH,000DH,000EH,000FH,0010H,0011H,0011H,0012H
FDB 0013H,0014H,0015H,0015H,0016H,0017H,0018H,0019H
FDB 0019H,001AH,001BH,001CH,001DH,001EH,001EH,001FH
FDB 0020H,0021H,0022H,0023H,0023H,0024H,0025H,0026H
FDB 0027H,0028H,0029H,0029H,002AH,002BH,002CH,002DH
FDB 002EH,002FH,0030H,0030H,0031H,0032H,0033H,0034H
FDB 0035H,0036H,0037H,0038H,0039H,003AH,003BH,003CH
FDB 003DH,003EH,003EH,003FH,0040H,0041H,0042H,0043H
FDB 0044H,0045H,0046H,0047H,0049H,004AH,004BH,004CH
FDB 004DH,004EH,004FH,0050H,0051H,0052H,0053H,0054H
FDB 0056H,0057H,0058H,0059H,005AH,005BH,005DH,005EH
FDB 005FH,0060H,0061H,0063H,0064H,0065H,0066H,0068H
FDB 0069H,006AH,006CH,006DH,006EH,0070H,0071H,0073H
FDB 0074H,0075H,0077H,0078H,007AH,007BH,007DH,007EH
FDB 0080H,0082H,0083H,0085H,0086H,0088H,008AH,008BH
FDB 008DH,008FH,0091H,0093H,0094H,0096H,0098H,009AH
FDB 009CH,009EH,00A0H,00A2H,00A4H,00A6H,00A8H,00AAH
FDB 00ADH,00AFH,00B1H,00B3H,00B6H,00B8H,00BBH,00BDH
FDB 00C0H,00C2H,00C5H,00C7H,00CAH,00CDH,00DOH,00D3H
FDB 00D6H,00D9H,00DCH,00DFH,00E2H,00E5H,00E9H,00ECH
FDB 00EFH,00F3H,00F7H,00FAH,00FEH,0102H,0106H,010AH
FDB 010FH,0113H,0117H,011CH,0121H,0126H,012BH,0130H
FDB 0135H,013AH,0140H,0146H,014CH,0152H,0158H,015FH
FDB 0166H,016DH,0174H,017CH,0183H,018CH,0194H,019DH
FDB 01A6H,01AFH,01B9H,01C4H,01CFH,01DAH,01E6H,01F2H
FDB 01FFH,020DH,021BH,022AH,023AH,024BH,025DH,026FH
FDB 0283H,0299H,02AFH,02C8H,02E2H,02FEH,031CH,033CH
FDB 035FH,0385H,03AEH,03DCH,040EH,0445H,0482H,04C7H
FDB 0514H,056BH,05CEH,0641H,06C7H,0766H,0823H,090CH
FDB 0A2DH,0BA2H,0D93H,104BH,145EH,1B29H,28BEH,517CH

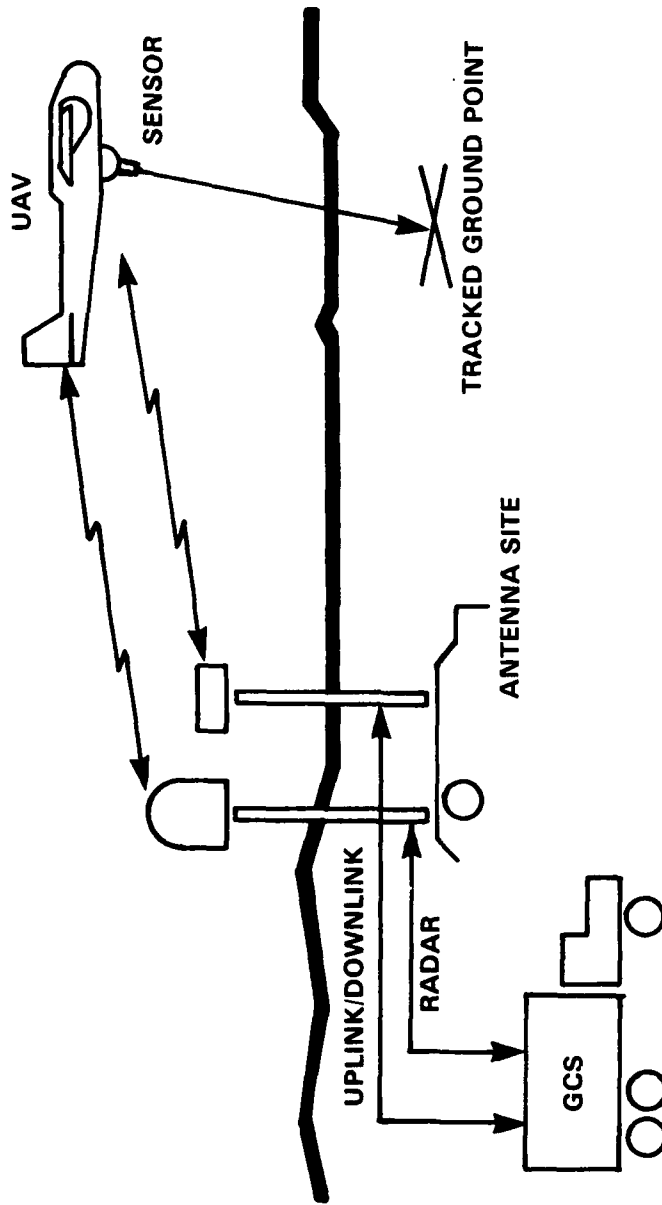


Figure 1
SURVEILLANCE UAV SYSTEM

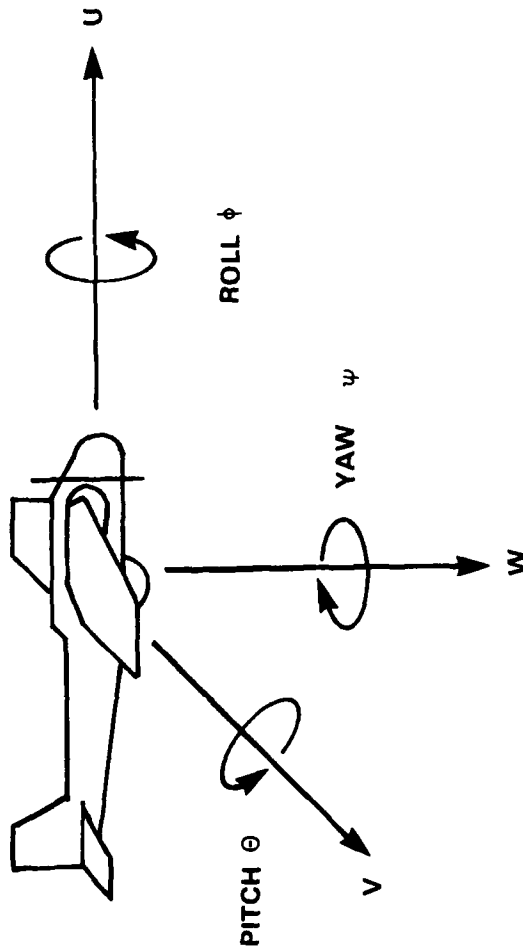
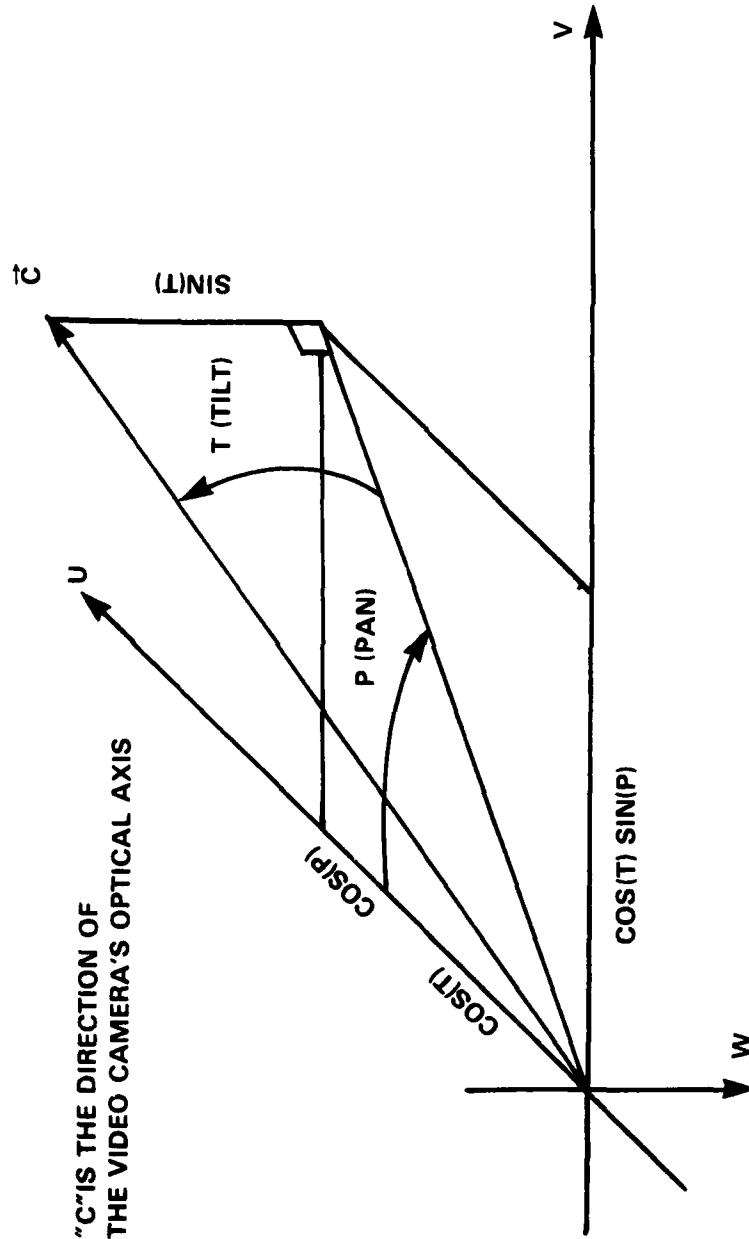


Figure 2
AIRCRAFT COORDINATE NOTATION



"C" IS THE DIRECTION OF
THE VIDEO CAMERA'S OPTICAL AXIS

Figure 3
SENSOR GEOMETRY

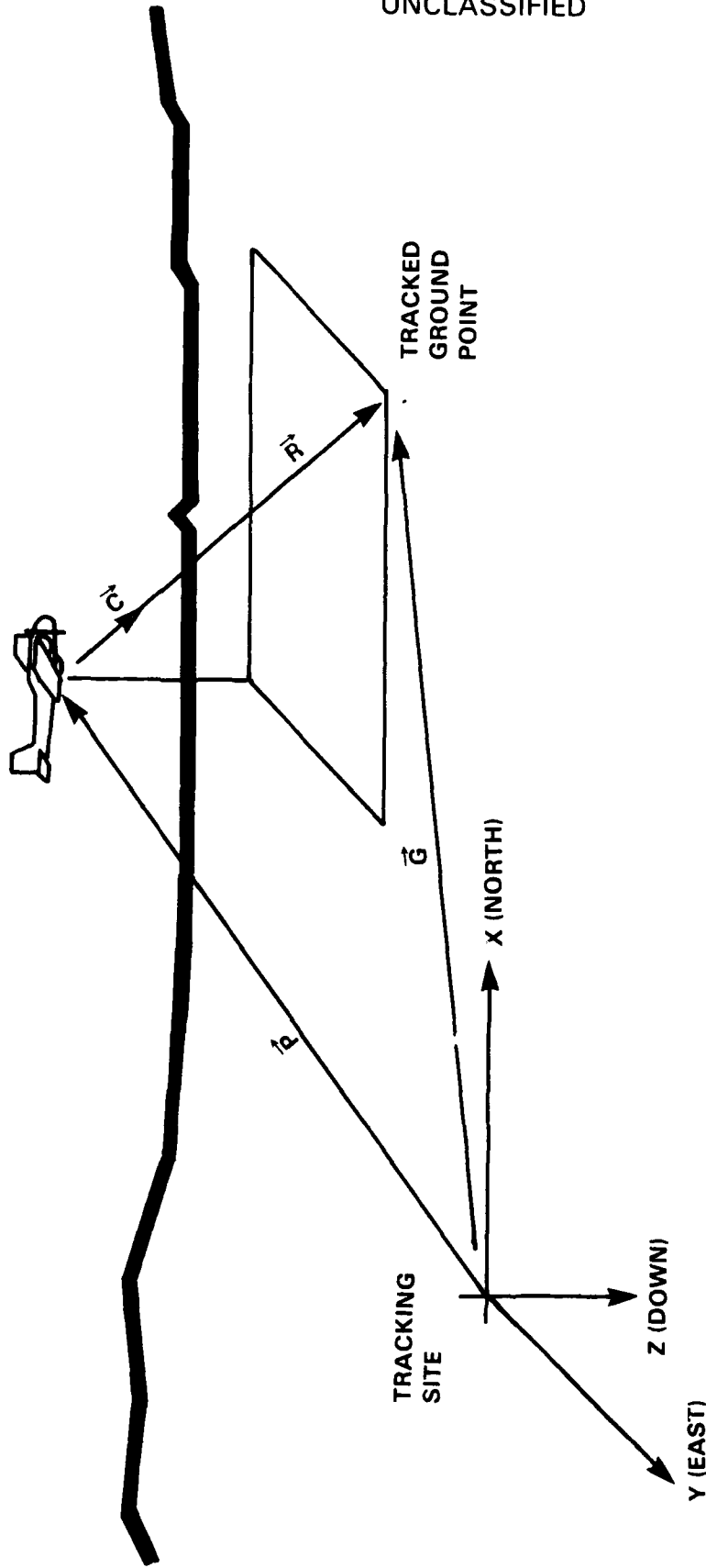


Figure 4
OVERALL GEOMETRY

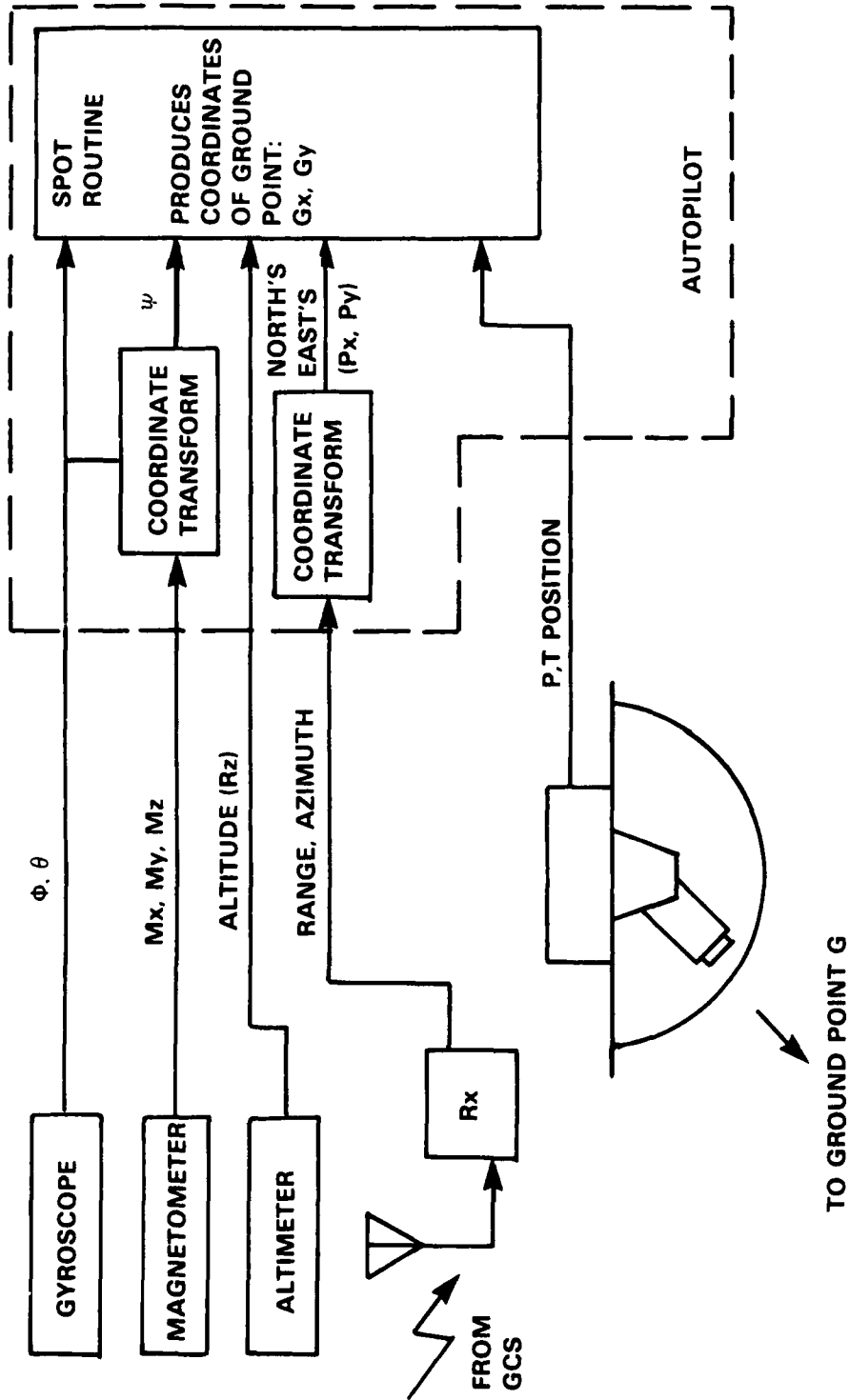


Figure 5
SPOTTING PROCESS

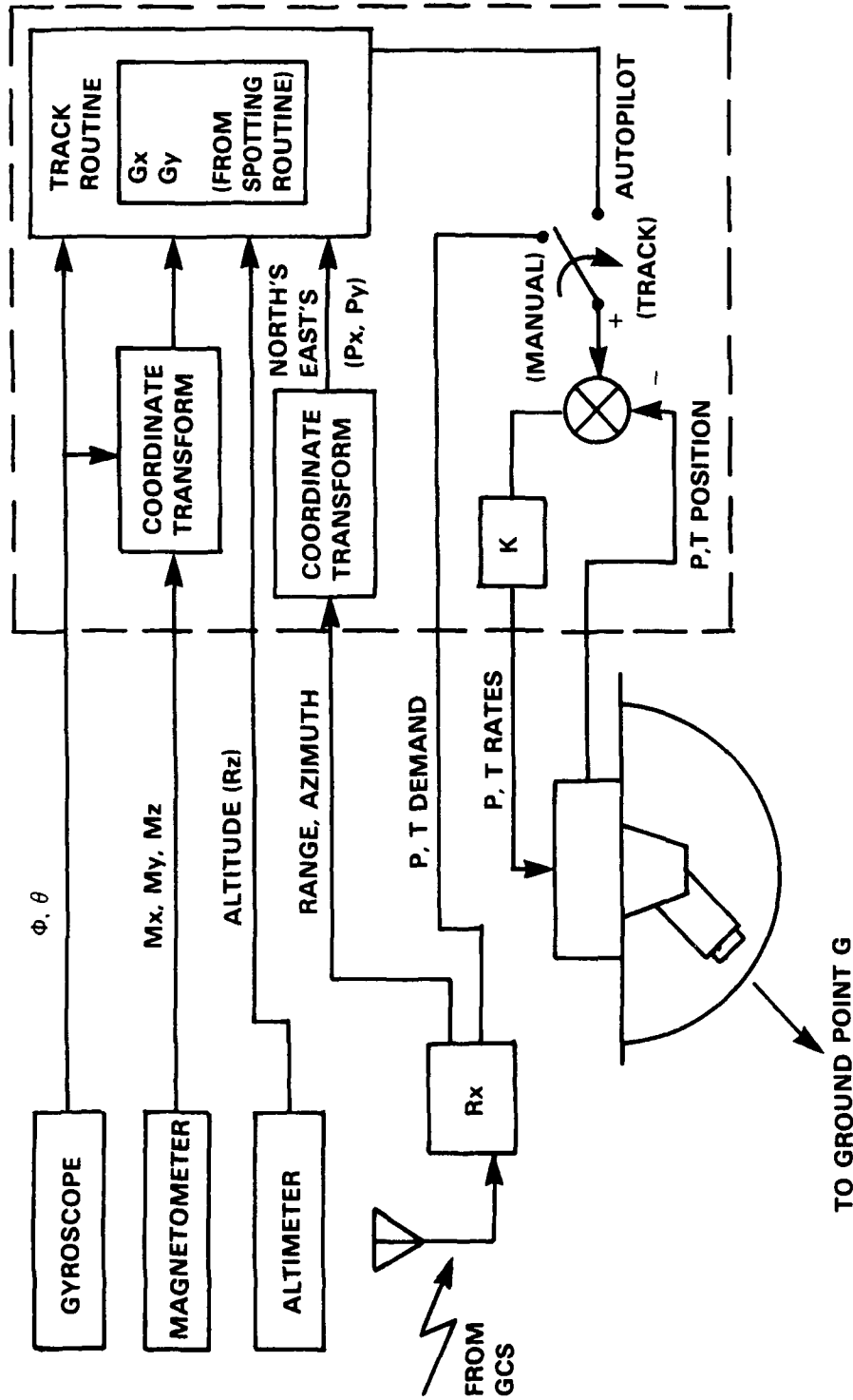


Figure 6
TRACKING PROCESS

UNCLASSIFIED

SECURITY CLASSIFICATION OF FORM
(highest classification of Title, Abstract, Keywords)

DOCUMENT CONTROL DATA

(Security classification of title, body of abstract and indexing annotation must be entered when the overall document is classified)

1. ORIGINATOR (the name and address of the organization preparing the document. Organizations for whom the document was prepared, e.g. Establishment sponsoring a contractor's report, or tasking agency, are entered in section 8.)		2. SECURITY CLASSIFICATION (overall security classification of the document, including special warning terms if applicable) Unclassified	
3. TITLE (the complete document title as indicated on the title page. Its classification should be indicated by the appropriate abbreviation (S,C,R or U) in parentheses after the title.) A Sensor Stabilization/Tracking System For Unmanned Air Vehicles (U)			
4. AUTHORS (Last name, first name, middle initial. If military, show rank, e.g. Doe, Maj. John E.) Decruyenaere, Jean-Paul R.			
5. DATE OF PUBLICATION (month and year of publication of document) May 1990	6a. NO. OF PAGES (total containing information. Include Annexes, Appendices, etc.) 34	6b. NO. OF REFS (total cited in document) 7	
6. DESCRIPTIVE NOTES (the category of the document, e.g. technical report, technical note or memorandum. If appropriate, enter the type of report, e.g. interim, progress, summary, annual or final. Give the inclusive dates when a specific reporting period is covered.)			
8. SPONSORING ACTIVITY (the name of the department project office or laboratory sponsoring the research and development. Include the address.)			
9a. PROJECT OR GRANT NO. (if appropriate, the applicable research and development project or grant number under which the document was written. Please specify whether project or grant)		9b. CONTRACT NO. (if appropriate, the applicable number under which the document was written)	
10a. ORIGINATOR'S DOCUMENT NUMBER (the official document number by which the document is identified by the originating activity. This number must be unique to this document.)		10b. OTHER DOCUMENT NOS. (Any other numbers which may be assigned this document either by the originator or by the sponsor)	
11. DOCUMENT AVAILABILITY (any limitations on further dissemination of the document, other than those imposed by security classification) <input checked="" type="checkbox"/> Unlimited distribution <input type="checkbox"/> Distribution limited to defence departments and defence contractors; further distribution only as approved <input type="checkbox"/> Distribution limited to defence departments and Canadian defence contractors; further distribution only as approved <input type="checkbox"/> Distribution limited to government departments and agencies; further distribution only as approved <input type="checkbox"/> Distribution limited to defence departments; further distribution only as approved <input type="checkbox"/> Other (please specify):			
12. DOCUMENT ANNOUNCEMENT (any limitation to the bibliographic announcement of this document. This will normally correspond to the Document Availability (11). However, where further distribution (beyond the audience specified in 11) is possible, a wider announcement audience may be selected.) Unlimited			

UNCLASSIFIED

SECURITY CLASSIFICATION OF FORM

13. ABSTRACT (a brief and factual summary of the document. It may also appear elsewhere in the body of the document itself. It is highly desirable that the abstract of classified documents be unclassified. Each paragraph of the abstract shall begin with an indication of the security classification of the information in the paragraph (unless the document itself is unclassified) represented as (S), (C), (R), or (U). It is not necessary to include here abstracts in both official languages unless the text is bilingual).

A control algorithm for the automatic steering of an imaging sensor has been developed at DRES. Both the tracking of a fixed ground point and the stabilization of the sensor are addressed. This system has been implemented in large part with pre-existing hardware and software in our UAV system. This report describes the theoretical basis of the system as well as detailing the issues concerning the development of a working prototype. *Remarks:*

Unmanned Air Vehicles,

14. KEYWORDS, DESCRIPTORS or IDENTIFIERS (technically meaningful terms or short phrases that characterize a document and could be helpful in cataloging the document. They should be selected so that no security classification is required. Identifiers, such as equipment model designation, trade name, military project code name, geographic location may also be included. If possible keywords should be selected from a published thesaurus. e.g. Thesaurus of Engineering and Scientific Terms (TEST) and that thesaurus-identified. If it is not possible to select indexing terms which are Unclassified, the classification of each should be indicated as with the title.)

UAV

Stabilization

algorithm

tracking RPV. *IRNIE*